Astroparticle Physics 124 (2021) 102505

Contents lists available at ScienceDirect

Astroparticle Physics

journal homepage: www.elsevier.com/locate/astropartphys

Stopping muon effect and estimation of intracloud electric field

A. Chilingarian[a,b,*], G. Hovsepyan[a], G. Karapetyan[a], M. Zazyan[a]

[a] Alikhanyan National Lab (Yerevan Physics Institute), Yerevan 0036, Armenia
[b] National Research Nuclear University MEPhI, Moscow 115409, Russia

ARTICLE INFO

Article history:
Received 26 March 2020
Revised 3 August 2020
Accepted 5 August 2020
Available online 7 August 2020

Keywords:
Cosmic ray muons
The atmospheric electric field

ABSTRACT

Employing large thunderstorm ground enhancements (TGEs) as a manifestation of the strong electric field in thundercloud we measure fluxes of almost all species of secondary cosmic rays to estimate the strength of the intracloud electric field. The modulation that electric field poses on charged particle flux gives a sizable change in count rate of detectors measuring high energy muon flux and inclined muon flux in the presence of a TGE. The muon stopping effect, observed by the particle detectors located at 3200 m altitude at Aragats Space Environmental Center (ASEC) implicates the abrupt decline of count rate of high energy muons (at vertical incidence with energies above 250 MeV and at inclined incidence with azimuth angle $\theta > 22^{\circ}$ for lower energies). For the large TGE events (relative enhancement $>$ 10% in SEVAN detector upper layer, registering low energy charged particles and electrons) muon count rate decreases down to 2-5% from the mean count rate measured before the TGE event. A simple model of shifting of the energy spectrum of particles entering the electric field was applied for the analysis of several events where the muon stopping (deceleration) effect has been observed. For the large TGE events that occurred during last decade the maximal potential drop of 350 MV was estimated. The most probable electric field strength for this event was found to be ~2 kV/cm.

1. Introduction

During thunderstorms, large synchronized impulsive enhancements in count rates of electrons, gamma rays, and neutrons have been observed by a variety of particle detectors [1–7]. These flux boosts, called thunderstorm ground enhancements (TGEs, [8]) imply that during a thunderstorm special conditions are established inside the cloud, leading to the modification (modulation) of the energy spectra of charged particles as well as to multiplication and acceleration of seed cosmic ray (CR) electrons. It is believed that these conditions are based on the presence of strong electric field, which accelerates or decelerates electrons, positrons, protons, and muons and, if the strength of the electric field exceeds the critical one, then the runaway breakdown (RB), also referred as relativistic runaway electron avalanche (RREA) are unleashed exponentially multiplying seed electrons number. The idea of runaway electrons in the atmosphere was suggested by C.T.R. Wilson in 1924 [9] and theory was developed in [10]. In RRE avalanche-accelerated electrons emit a large number of gamma rays via bremsstrahlung, gamma rays, in turn, produce neutrons by photonuclear reactions with air molecules. Along with the detection of a TGE, usually, the simultaneous decrease in the flux of high-energy muons was observed [11,12]. The positive to negative atmospheric muon ratio is measured to be 1.2-1.3 below 100 GeV/c [13,14]. Therefore, the overall muon flux can be reduced due to the deceleration of positive muons by the atmospheric electric field. This effect has been theoretically analyzed in several papers [4,15,16], however, the estimates of the decrease in muon flux fail to explain the muon flux decrease measured at Baksan Astrophysical Observatory [17]. An alternative model was presented in [18] where the decline of muon flux was related to the limited lifetime of muons from the generation at ~15 km above sea level till observation level at lower altitude. Strong fields, as a rule, have a layered structure with alternating field polarity [19–23]. If due to charge separation large uncompensated potential arises in the thundercloud near the earth's surface (common case for TGE) it will lead both to the large increase in the fluxes of electrons and gamma rays, and to the decrease of the high-energy muon flux [24].

At the Aragats Space Environmental Center in 2009 [25] we routinely measure TGE events, observing significant enhancements of electron and gamma ray flux simultaneously with enhancement of neutrons and drop of muon flux (positive muons are declined by the same intracloud electric field that accelerated electrons downward in the direction of Earth, see for instance Fig. 4 and Tab. 3 of [26]. In [27] we estimate the size of the emitting region in the thundercloud by registration of the muon flux depletion under large zenith angles. In the present paper, we perform analysis of

* Corresponding author.
E-mail address: chili@aragats.am (A. Chilingarian).

https://doi.org/10.1016/j.astropartphys.2020.102505
0927-6505/

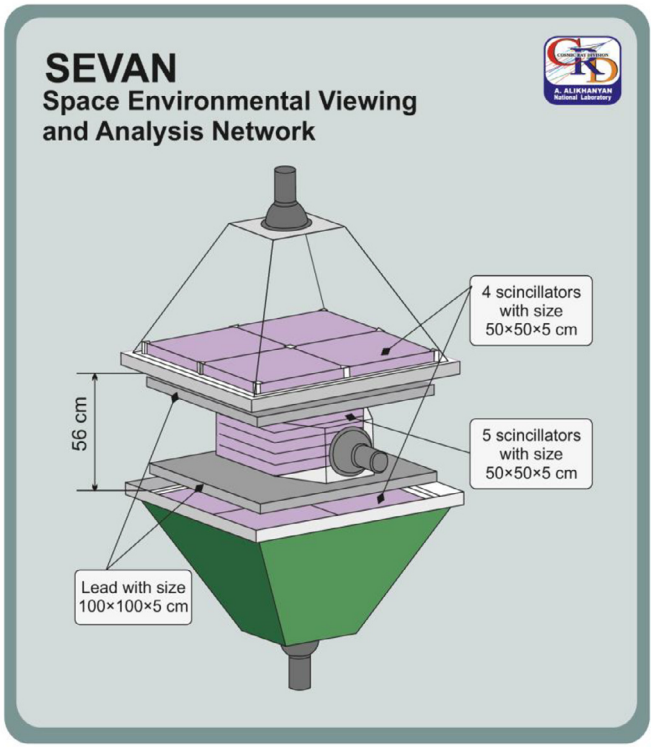

Fig. 1. The module of the European "Space Environmental Viewing and Analysis Network" (SEVAN).

the particle fluxes modulated by the atmospheric electric field and estimate the maximal potential drop and the maximal strength of the electric field based on the large TGEs measured by the SEVAN detector. In present paper we will call "large" TGE, the TGEs that demonstrate a more than 10% enhancement in the 1-minute count rate time-series measured by the 5 cm thick and 1 m^2 area plastic scintillator (upper scintillator of SEVAN detector).

2. Registration of TGEs with SEVAN and other particle detectors on Aragats

Observational data from Aragats particle detectors demonstrate several remarkable TGE events, usually accompanied by the muon flux decrease. In Fig. 1 we show the chart of a SEVAN detector belonging to European space environmental viewing and analysis network [28]. SEVAN is assembled from standard slabs of plastic scintillators of $50\times50\times5cm^3$ size. Between 2 identical assemblies of $100\times100\times5$ cm^3 scintillators (4 slabs) are located two $100\times100\times4.5$ cm^3 lead absorbers and thick $50\times50\times20$ cm^3 scintillator assembly (5 slabs). The data stream from the SEVAN comprises 1-minute count rates from 3 stacked scintillators. All combinations of signals from detector layers are stored as well: "100" combination means that the signal was only in the upper layer; "111" – that signal comes from all 3 layers, etc.

Different combinations of SEVAN coincidences effectively select various particles from the cosmic ray flux. The combination "100" for example, means low energy particles; the combination "010" – mostly neutral particles; combinations "111" and "101" – high energy muons. The purity of particle selection by SEVAN coincidences was estimated by simulations, see Fig. 4 in [28]. The purity of muon selection is rather high ∼95%, due to a 10cm lead filter to be traversed by the particle. The energy threshold of the upper detector due to the matter of the roof (1 mm thick metallic tilts and 3 cm thick wooden bricks) above and detector housing matter is ∼ 7 MeV. The minimum energy of muons to be detected in all three layers is ∼250 MeV.

Table 1
The mean values, variances, and relative errors of SEVAN, and Neutron Monitor one-minute count rates and ASNT 10-sec time count rates measured at 17:40-18:10, on 4 October 2010 in fair weather. Peak of the flux in natural value and in percent occurred at 18:23 (deficit of muons).

Detector	Mean	σ	Re (%)	Peak	%	Nσ
Neutron Monitor	32249	237	0.7	34127	5.8	7.9
SEVAN Coinc.111	2691	51	1.9	2546	-5.6	-2.9
SEVAN Coinc.100	16586	130	0.8	27228	65	82
SEVAN Coinc. 010	2040	39	1.9	3487	70	37
ASNT 4 m.sq. (10s)	16530	133	0.8	34204	107	133
ASNT vertical	2192	46	2.1	2383	8.7	4.2
ASNT Coinc. 2-8+1-7	506	23	4.5	476	-5.9	-1.3

In Fig. 2 we show the one-minute time-series of particle fluxes before, during, and after the TGE occurring on 4 October 2010. The TGE was sustained for ∼ 7 minutes and exhibits a large peak at 18:23 (Tab. 1). Due to the large difference in the count rates of various detectors the natural count rate scale is not illustrative (Fig. 2a): the deviations from the mean count rate are not well pronounced for time series with a low count rate. Thus, to emphasize and digitize the significance of enhancements (peaks) we present time series not only in natural units but also in percent (Fig. 2b), and in units of the number of standard deviations from the mean count rate (Nσ) measured before the enhancement at fair weather (Fig. 2c). The mean values and variances for all detectors used were estimated during one and the same time 17:40-18:10, see Table 1. Mean and peak values, variances, and peak significances (Nσ) are in natural numbers; the relative abundances (%) and relative errors (Re) – in percent. The count rates shown in percent (Fig. 2b) do not reflect the differences in accuracy of particle detectors; the time series shown in number of standard deviations (Nσ, Fig. 2c) give the possibility not only to estimate the chance probability (significance of enhancement), but also to compare the "strength of evidence" provided by different detectors. In Table 1 we show the significances of the peaks in time-series of count rates measured by various detectors and combination of registered signals in SEVAN detector layers. From Fig. 2c and Table 1 we can see that low energy particles (red, coincidence "100"), neutral particles (green, coincidence" 010", mostly gamma rays), and neutrons (black) demonstrate significant enhancement in the number of σ. The chance probability of enhancement to be a background fluctuation even for the smallest enhancement (neutrons) is vanishingly small.

The 65% flux enhancement (significance 82σ is due to penetrating electrons and gamma rays) from the RRE avalanche developed in the thundercloud just above the building where the detector is located [8]. The counts of the standard neutron monitor 18NM64, located nearby the SEVAN detector, show a 5.8% increase. For the same time interval, the "111" combination demonstrates a pronounced decrease of counts (∼5.6%). By getting secondary fluxes at 3200 m from the WEB calculator EXPACS [29] one can deduce that particles initiating these counts represent mainly muons (purity of muon selection by "111" combination of SEVAN is ∼95%).

In Fig. 3 we present the pattern of the near-surface electric field disturbances during the TGE event of 4 Oct 2010 along with enhancement of the count rate measured by the large plastic scintillators of the Aragats solar neutron telescope (ASNT, occurred at 18:22:50, see Fig. 5, 10-second time series). In Figs. 2c and 3 one can see that the peaks measured by SEVAN and ASNT detectors occurred simultaneously and that due to larger size, the relative enhancement measured by ASNT is two times larger than measured by the SEVAN "100" combination. The significance of the 1-minute time series equivalent of ASNT is outstanding, exceeding 300 σ!

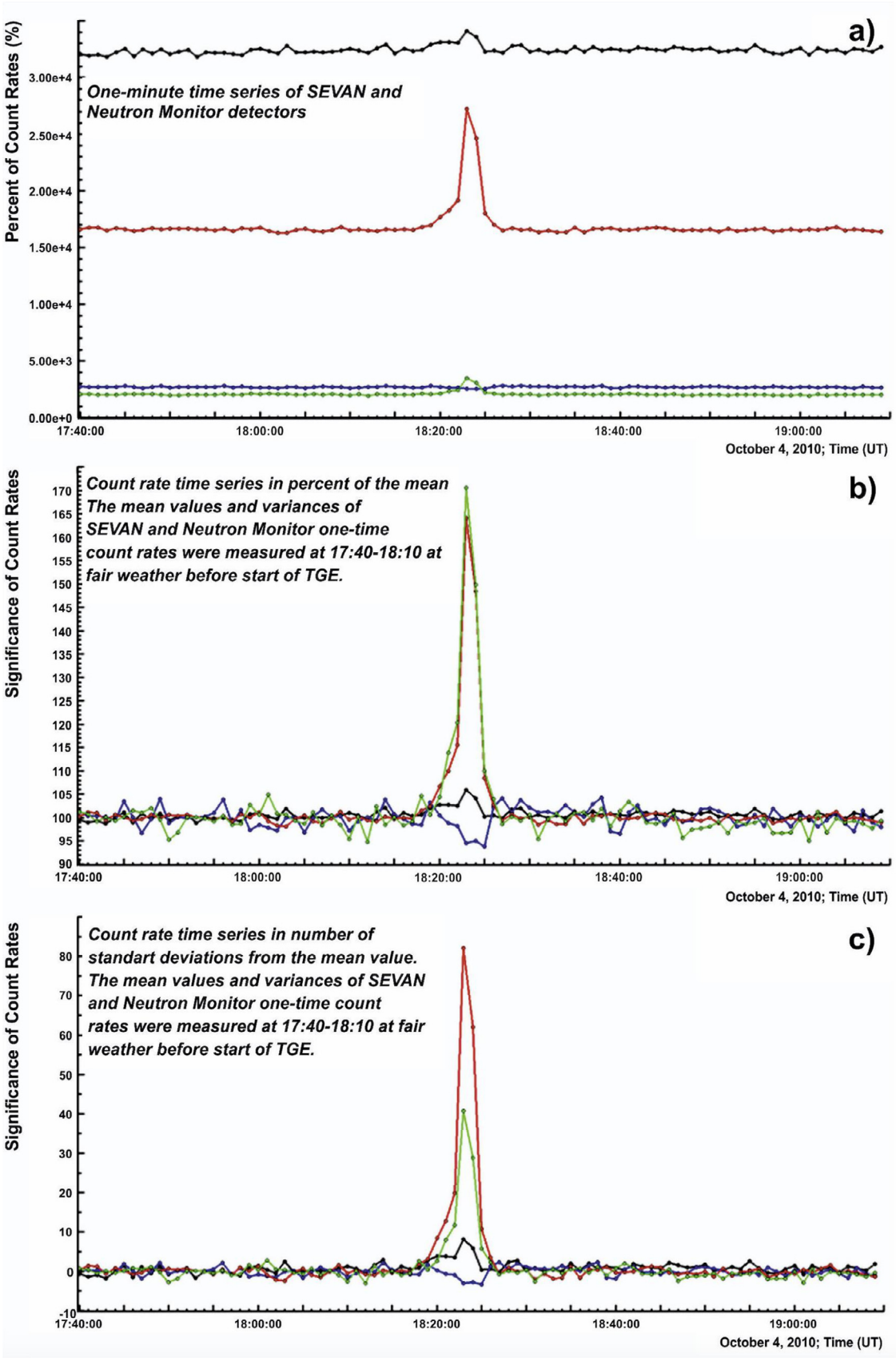

Fig. 2. Time series of the SEVAN detector count rates: muons (combination "111", blue), electrons (combination "100", red), gamma rays (combination "010", green), and neutrons (measured by the Neutron Monitor 18NM64, black). In a) we show the particle fluxes in number of counts per minute; in b) – particle one-minute flux in the percent to the fair-weather flux measured before the TGE; in c) the same flux but measured in the number of standard deviations, the one-minute mean and variance of the flux were calculated from the time-series measured in fair weather before TGE.

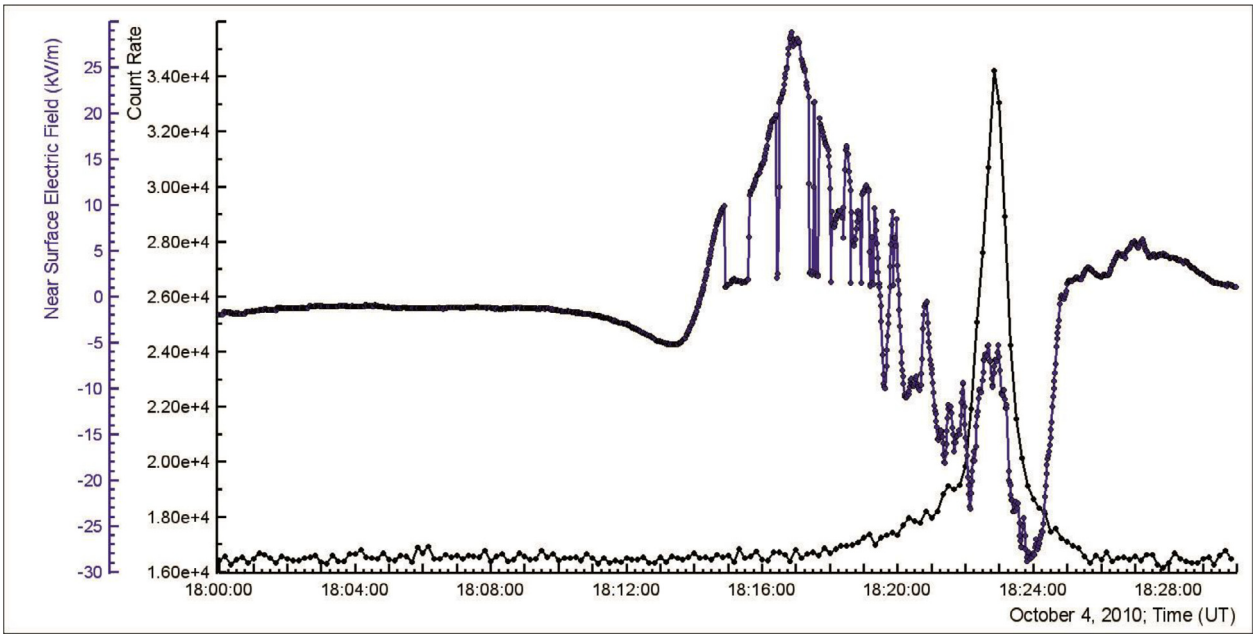

Fig. 3. Near-surface electric field disturbances measured by the electric mill EFM-100 of BOLTEK firm and enhancement of the 20-sec count rate measured by 4 m^2 and 5cm thick plastic scintillator of the ASNT detector.

The impulsive increase of particle flux happened during negative near-surface electric field when a brief outburst of the strength of the electric field was directed to the positive field domain. The model of the TGE event identifies such a burst as the emergence of a lower positive charge region in the bottom of the cloud, which significantly enlarges the strength of the intracloud electric field and initiates large TGEs (see Fig. 1 in [30]). The large intracloud electric field leads to the enormously large maximal energy of TGE electrons (≈50 MeV) measured by the 60 cm thick scintillator of the ASNT detector (Fig. 11 in [31]). Energy spectra of electrons and gamma rays observed simultaneously with the TGE ~5.6% deficit of muon flux (blue curve in Fig. 2), is another evidence of a large intracloud electric field that accelerates electrons and negative muons respectively and decelerates positive muons.

To estimate quantitatively the strength of the electric field, we develop a simple model, based on the modification of energy spectra of different species of CRs due to traversal through the electric field of the thundercloud.

3. Description of model for inferring the intracloud electric field

Suppose that muon detector has a threshold E_t and that before detecting the traverse of muons throw the net potential drop V (we assume that the electric field in the cloud accelerates electrons and negative muons in the downward direction to Earth and decelerates positive muons). In the presence of an electric potential V, positive muon energies will change by a value U=eV, so that number of positive muons, contributing to the count rate will be $I_{m+}(E_t+U)$, and the number of negative muons correspondingly - $I_{m-}(E_t-U)$, where I(E) is the integral spectrum, giving the number of particles with energy >E (i.e. the count rate of the detector) at 3200 m, the altitude where the SEVAN detector is located. Due to this transformation, the flux of accelerating negative muons will increase, and the flux of decelerating positive muons – decrease. A total change of the count rate F(U) is determined by the increase of negative muons and decrease of positive muons:

$$F(U) = 100\frac{f(U) - f(0)}{f(0)}, \quad (1)$$

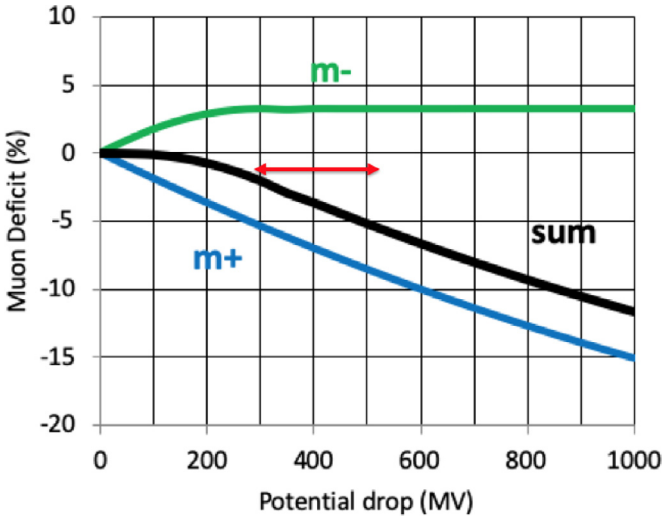

Fig. 4. Modulation of particle count rates by the electric field; energy threshold of SEVAN "111" combination (95% muons) ~ 250 MeV. Curves correspond to Eqs. (1) and (2) for flux changes of different species of CR dependent on the potential drop V. By double-sided arrow we denote the potential drop region corresponding to the muon depletion values measured by the SEVAN detector on Aragats.

$$f(U) = I_{m+}(E_t + U) + I_{m-}(E_t - U) \quad (2)$$

where indexes m+, m- correspond to positive and negative muons. To calculate integral spectra, we use the EXPACS WEB calculator, results are presented in Fig. 4.

Curves in Fig. 4 represent the percent of change in muon flux in electrified conditions relative to storm-free conditions. As we can see in Fig. 4 after a potential drop of 300 MV the increase of negative muon flux stopped. This is because the existent portion of low energy muons from cosmic ray flux has already gained energy from the electric field and has energy above 200 MeV. The numbers of positive muons continue to decrease with increasing potential drop. As a result, the deficit in the detector's count rate will be

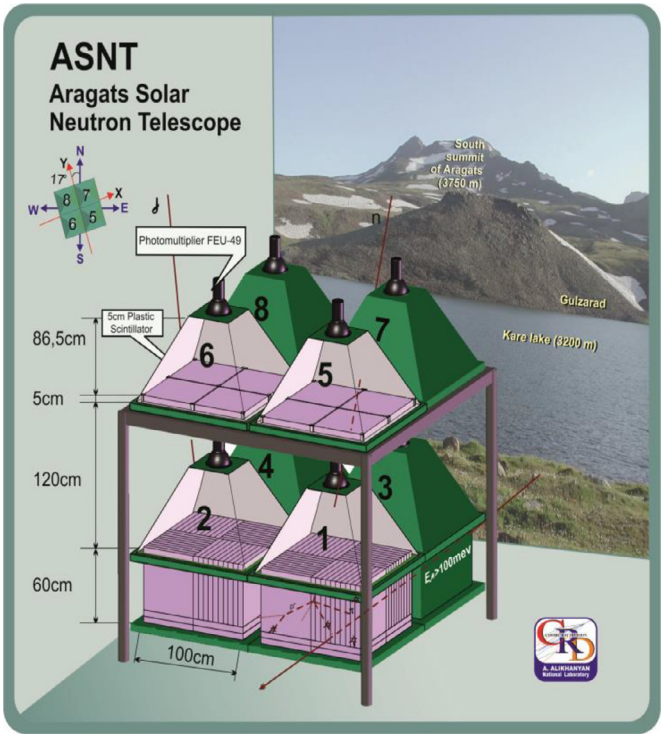

Fig. 5. ASNT detector assembly; near vertical flux is measured by coincidences 1-5, 2-6,3-7, 4-8; inclined flux direction – by 1-7 and 2-8.

proportional to the deficit of positive muons. Thus, as seen from Fig. 4 we estimate for a net potential drop 400 MV expected muon deficit of 3.8% and, for the observed 4 October 2010 5.6% deficit - slightly above 500MV.

4. Inclined muon trajectories during TGE

The large variety of particle detectors operated at Aragats gives possibility to measure one and the same event with independent facilities and investigate correlations between different species of cosmic rays. As usual, the muon stopping effect was checked with another particle detector operated on Aragats. The Aragats Solar Neutron Telescope (ASNT, see detailed description in [32]) registers both near-vertical and inclined fluxes of CR particles. The ASNT comprises 4 separate identical modules, as shown in Fig. 5. Each module consists of standard slabs of $50\times50\times5$ cm^3 plastic scintillators stacked vertically on a $100\times100\times10$ cm^3 horizontal plastic scintillator slab.

A near-vertical flux (0-20°) is composed of the particles, which are registered by the pairs of scintillators (1,5), (2,6), (3,7) and (4,8). Inclined fluxes are registered by other pairs of scintillators i.e. combinations (1,7) and (2,8) coincidences correspond to the inclined direction at a zenith angle (20-60)°.

The energy threshold of the upper 5 cm thick scintillators is ~5 MeV. Count rates corresponding to the near vertical and inclined muon incidences are shown in Fig. 6. The count rate dynamics of the near-vertical and inclined particles during TGE are dramatically different. If we observe a sizable enhancement in the near-vertical direction (expected arrival direction of the TGE particles), at the same time on the same detector using the same DAQ electronics and analysis software we measure a deficit in the inclined particle flux (significant fraction of muons enters the ASNT under large zenith angles). The measurement of TGEs on Aragats in the last decade demonstrate that the height of the thundercloud base usually is 25-150 m (corresponding to a location near the freezing temperature (0 C) in the lower part of the cloud) for the largest TGE events. Thus, bremsstrahlung gamma rays enter detectors mostly from the near-vertical direction. In contrast, CR particles from extensive air showers (EASs, the source of CR muons) that start well above the detector site (~10 km) have much broader angular distribution and are entering particle detectors under large zenith angles as well. Measuring inclined particle trajectories (mostly muons), we can avoid the overwhelming contribution of TGE particles accelerated by the vertical electric field and seen in the near-vertical direction (Fig. 6, black curve). The muon stopping effect is apparently seen in Fig. 6, because the blue curve goes down at the same time the near-vertical flux (black curve) is enhanced. The pronounced decreases of the count rate of inclined trajectories at ~18:20 - 18:24, coincide with a muon count rate decrease in the SEVAN detector (Fig. 2). The statistical significance of the measured deficit is low due to larger fluctuations of inclined particle fluxes; however, it coincides well in time with the deficit measured by the SEVAN 111 combination and with the enhancement of count rate of particles coming from the vertical direction measured by the same detector. Thus, the ASNT observations provide additional evidence of muon deceleration effect.

Almost the same pattern of the muon stopping effect was observed on 21 May 2009, see Fig. 7. However, on 21 May the TGE was weaker compared with that of 4 October TGE (gamma ray and electron enhancement were ≈14%, on 4 October 2010 – 60%). Flux enhancement measured by the "100" combination of SEVAN reaches only ~17%; neutron flux enlarged by ~3% and muon flux declines by ~3%, as we can see in Fig. 7. The inclined muon flux, again demonstrated depletion (Fig. 8).

5. Meteorological conditions supporting emergence of the strong atmospheric electric field that modulates particle fluxes registered on the earth's surface

In the Aragats events database we select several TGEs large enough to observe the muon flux deceleration. The selection was performed according to condition that the enhancement of the "100" combination of SEVAN detector (signal was registered only in upper scintillator, energy threshold 7 MeV) be larger or equal to 9% of the mean flux measured before the TGE. To get insight in the atmospheric conditions supporting the emergence of the electric field in the atmosphere we analyze these events along with meteorological conditions and near-surface electric field records. Typical TGE events observed in 2012-2015 are shown in Figs. 9 and 10 and enumerated in Table 2. Frames a-d in the Fig. 9 demonstrate enhanced electron – gamma ray fluxes and suppression of the muon fluxes. The electric field during events was highly disturbed, as we can see in Fig. 10. All 4 TGE events occurred at rather narrow outside temperatures -0.8 – 2.2 C° (from the start to the end of TGE according to the time-scale in frames a-d in Fig. 10, see details in Table 2). And for all 4 TGE events the temperature is descending from the start to the end of TGE. The freezing level is above near the cloud base and a local positive charge is located precisely there at the freezing level [19], where charge reversal become possible. Thus, temperature appears to be the most important parameter in controlling the charge structure [22], and, in particular, in the creation of the lower dipole that accelerates electrons downward. The same dipole will decelerate positive muons and reduce total number of counts registered by the "111" combination of SEVAN detector.

Another demonstration of the intensification of the electric field is the graupel growth and fall in the form of snow pellets just before the TGE. In Fig. 11 we show the shots of the panoramic camera located on the roof of the MAKET experimental hall. We monitor skies above Aragats making shots each minute (now at high near-surface electric field – each second). Sometimes before and

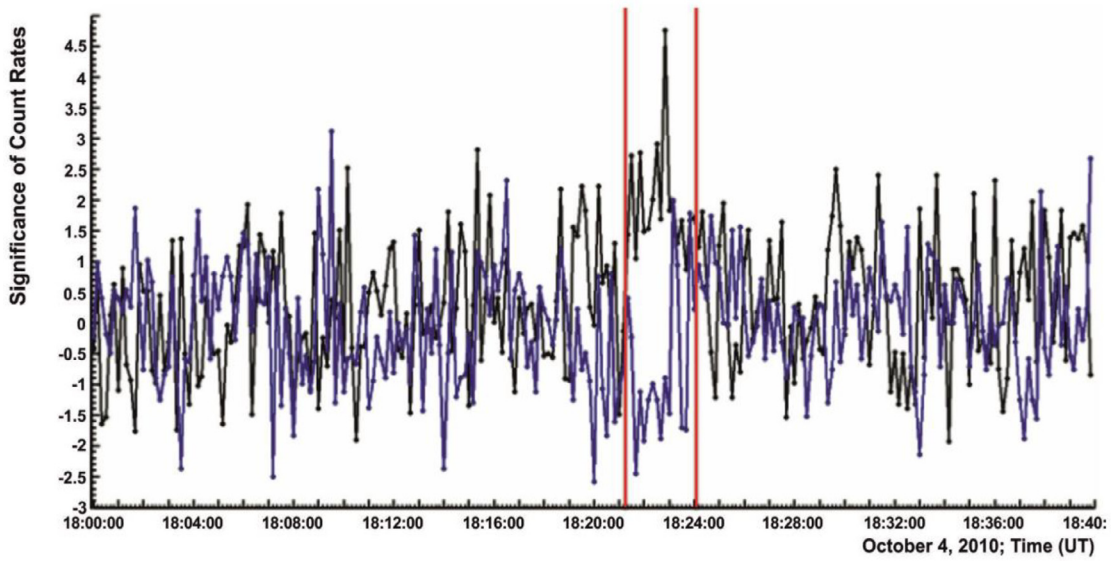

Fig. 6. 10-second counts of ASNT from near vertical direction (black) and, inclined direction (blue). By red lines we denote time span of muons with inclined paths and muons with near-vertical paths.

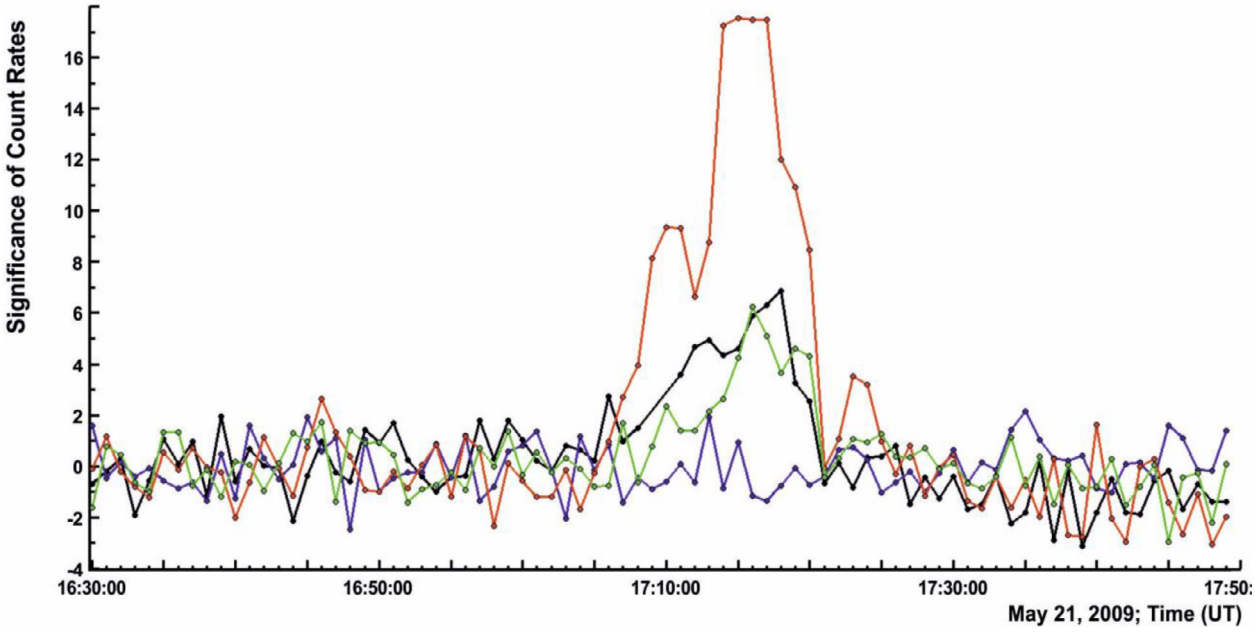

Fig. 7. Time series of the SEVAN detector: blue - muons, combination "111", -3% (-1.3σ); red - low energy gamma rays and electrons, combination 100, 14% (17σ); green – mostly gamma rays, combination 010, 18% (6.3σ); black - neutrons (18NM64), 3.6% (6σ).

Table 2
Characteristics of the TGEs shown in Figs. 9 and 10.

Date	Muon deficit [%]	Electron & gamma ray boost SEVAN/STAND1[%]	El. field record [kV/m]	Cloud base height [m]	Outside Temp. interval [C°]	RH [%]
a) May 13 2012, 19:24	-4.4	9.3/22	-30 - - 16	65	0.4 - -0.5	95
b) May 27 2014, 9:02	-4.6	12.3/31	-17 - +5	60	1.9 -0.2	94
c) Sept. 30 2014, 13:02	-3.5	19/65	-11 - +5	95	1.9 – 0.4	94
d) May 11 2015 10:45	-2.5	11/36	-24 - +29	130	2.2 – 1.4	92

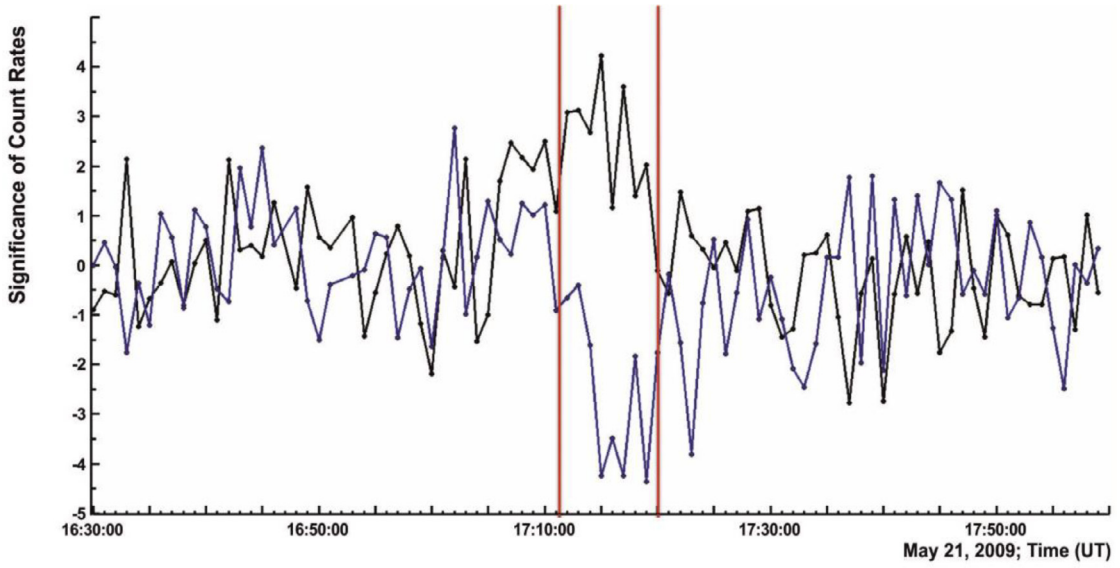

Fig. 8. One-minute counts of the ASNT from near-vertical direction (black) and inclined direction (blue). By red lines, we denote the time span of muons with inclined trajectories relative to the vertical (17:11 – 17:20).

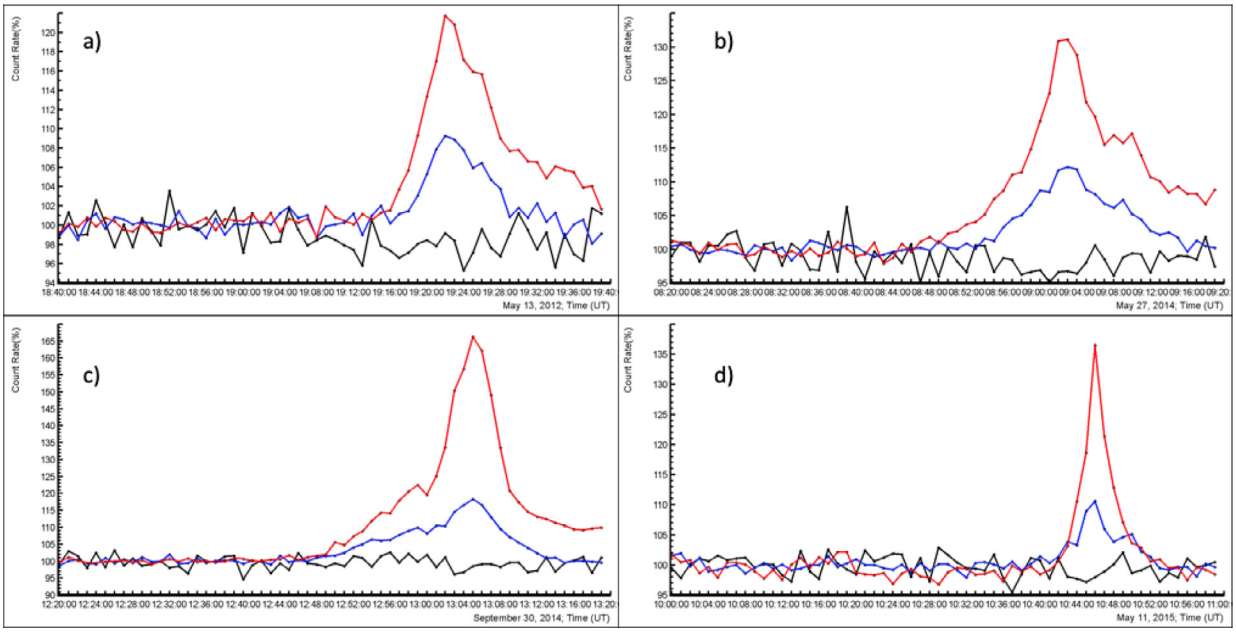

Fig. 9. Registration of the electron – gamma ray avalanches (RREA) and depletion of the muon flux during large TGEs occurred on May 13 2012 - a); May 27 2014 - b); on September 30 2014- c); and May 11 2015 – d). Black curves - SEVAN 111 - combination, muons with energies above 250 MeV; blue curves – SEVAN 100 combination, particles with energies avove 7 MeV, red curve – count rate of 1 cm thick upper scintillator of the STAND1 detector, energy threshold – 1 MeV.

during TGE graupel is reaching earth's surface; the hydrometeors fallen on glass of the camera didn't melt immediately and we got very special patterns, see Fig. 12. The staff of the station on March 31 2020 made photographs of the graupel on the earth's surface. The graupel fall started at 16:10-16:20 then changed to snow and again to graupel at 17:05 just before start of TGE at 17: 15 (reaching maximum at 17:58). On the panoramic camera shot, we show graupel of the specific conical shape, see Fig. 13. Thus, we confirm Kuettner's conclusion that a pocket of positive charge (LPCR) in the base of cloud is attached to precipitation and with the main negatively charged layer (located at 5000-6000 m MSL [33]) formed a "Graupel dipole" in the lower part of the cloud [19]. The developed LPCR significantly changed the near-surface electric field from deep negative to positive values, see Fig. 10 and Table 2. The amplitude of the field excursions in a few minutes can reach several tens of kV/m. The particle flux increases simultaneously with the emerging of LPCR.

Not only intensity, but also maximal energy of TGE electrons and gamma rays (reaching 40-50 MeV) can be taken as evidence for the large electric field in the cloud [30]. In Fig. 13 we show energy spectra of 2 events from 4 posted in Figs. 9 and 10 and in Table 2, namely events a) and c) obtained with network of NaI spectrometers located on Aragats (see details the spectrometer operation in [32]). The maximal energy was reached just during the minute of the maximal depletion of the muon flux at 19:24 (13 May, 2012) and at 9:02 (27 May 2014).

Thus, large enhancement of the intensity of the gamma ray and electron fluxes, large maximal energy of gamma rays, and electrons and muon deficit, all evidenced strong electric field in the cloud. As we can see in Fig. 13 and Table 2, maximal energies (20 and 40

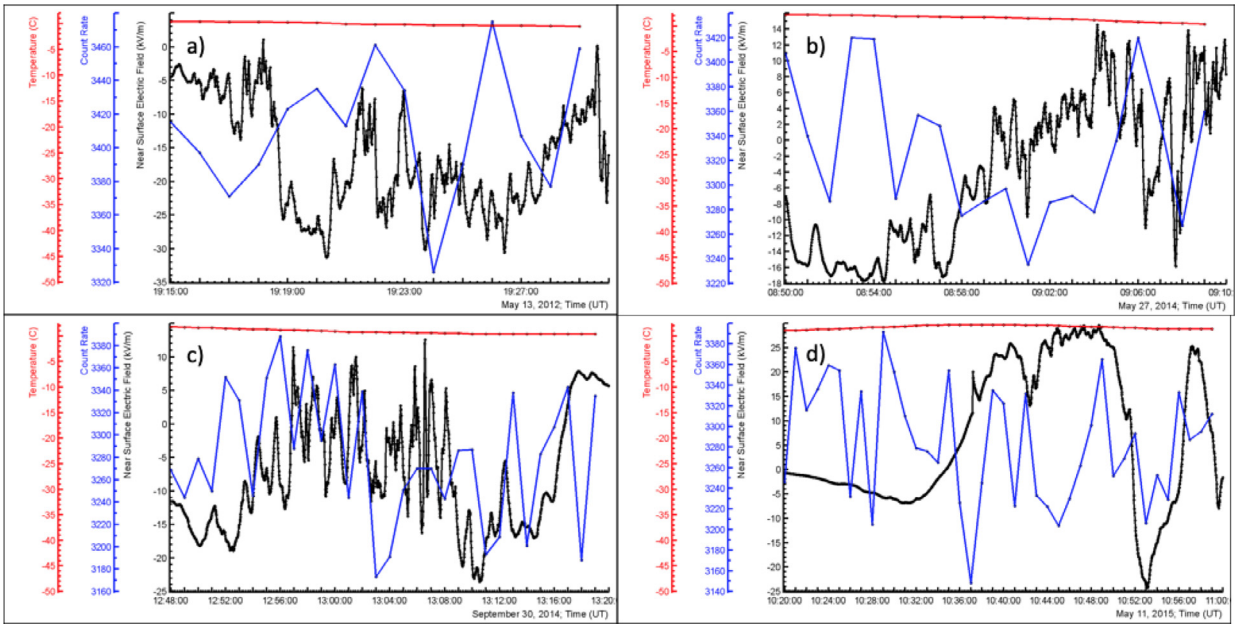

Fig. 10. Record of the near-surface electric field during TGE (black curve), muon flux depletion (blue curve, correspondent to frames a-d of Fig. 9); and outside temperature (red lines) for four selected events: a) May 13, 2012; b) May 27, 2014; c) September 30, 2014; d) May 11,2015. The parameters shown in Fig. 10 are presented in Table 2.

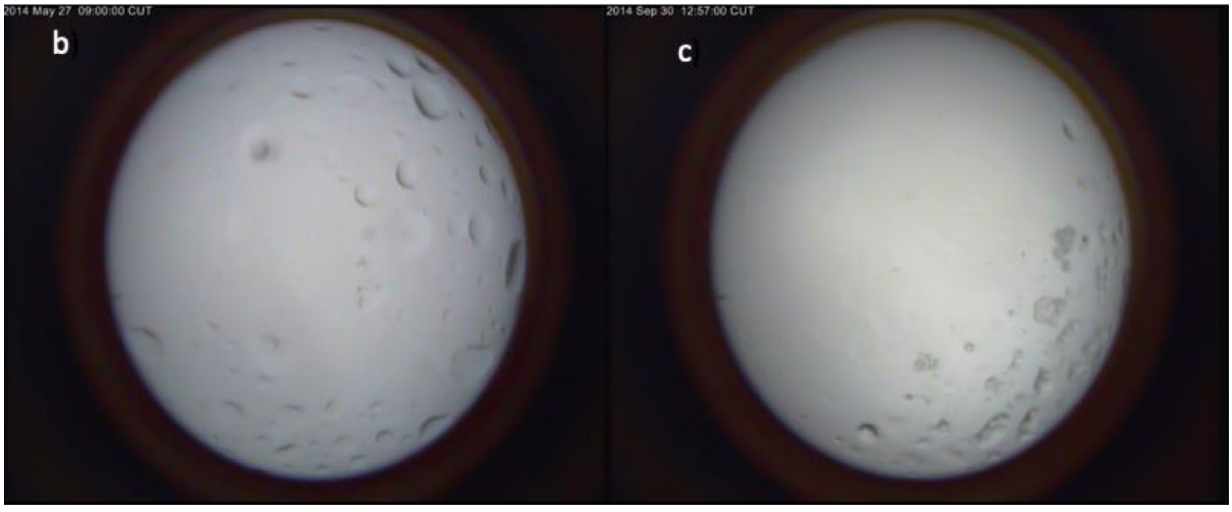

Fig. 11. Shots of the panoramic camera located on Aragats made before start of TGEs observed on May 13 and September 30 2014 (frames b and c in Figs 9 and 10).

MeV) are well related to the muon flux drop (-4.4% - -4.6%) of the analyzed events.

6. Propagation of the secondary species of cosmic rays through the extended atmospheric electric field (a simulation study)

To check the potential drop – muon deficit relation obtained with a simple EXPACS WEB calculator [29] we perform a simulation study with CORSIKA code [34] using QGSJET [35] model for high-energy hadronic interactions and UrQMD [36] model at low energies. The electromagnetic interactions were simulated with the EGS4 [37] model. The CORSIKA version 7.7400, which takes into account the effect of the electric field on the transport of EAS particles was used in this simulation work. In the simulation trials, we follow all species of extensive air shower (EAS) from the first strong interaction high in the terrestrial atmosphere including all secondary interactions until the muon arrival to SEVAN detector at 3200 m. The simulations were implemented for primary protons at the energy range from 10 to 1000 GeV within zenith angles from 0 to 50°. The energy spectrum of primary protons was generated according to the power law with spectral index -2.7. The shower particles were followed until the energy decreases to 300 MeV for hadrons and 100 MeV for muons, electrons, and photons. Each simulation trial includes 10^5 events.

The extent of the electric field varied from 1 to 2 km above particle detectors. The largest TGEs occurred on Aragats when the distance to the cloud base (a proxy of electric field lower boundary) was 25 – 50 m. Using data from satellite measurements as an input to the weather research and forecasting model (WRF) the electrifications processes above Aragats was studied during some of largest TGEs [38]. Runaway electrons were accelerated in the lower dipole formed by the well pronounced lower positive and middle negative layers separated by distances of 2 – 3.5 km [38].

If we assume this or smaller values of the field extent, the corresponding strength of the electric field will be from 1.8 to 2.2 kV/cm in good agreement with simulations with CORSIKA and GEANT4 codes [39]. Thus, the electric field was introduced in simulations from 3225 to 4325, 4725, and 5225 m. The simulation of

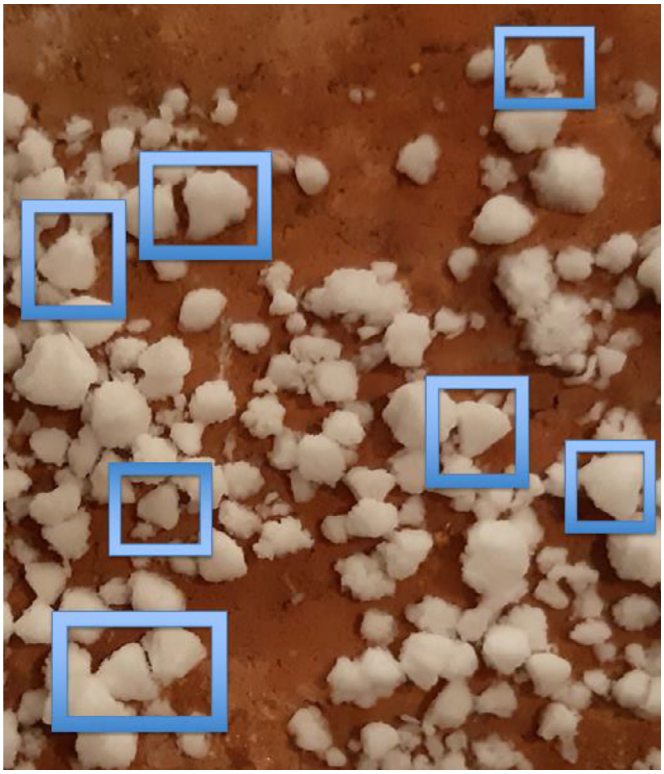

Fig. 12. The "conical" graupel fallen before TGE outlined by the frames, Aragats, March 2020

the relativistic runaway electron avalanches (RREAs) was done with the same electric field parameters according to the scheme described in [40]. Simulations were performed with an electric field of 1.8 - 2.2 kV/cm spread uniformly above Aragats station. The uniform electric field accelerates negative muons and electrons and decelerates positive muons and positrons. We use seed electron beams with constant energy of 1 MeV to suppress the contamination of the MOS process (modification of electron energy spectra, see details in [31,36]. Each simulation trial includes 10^4 events.

As it was demonstrated by CORSIKA and GEANT4 simulations [31,40] RREA is a threshold process and avalanches started at reaching the breakeven value of the atmospheric electric field. The length of the electric field also should be enough prolonged to allow cascade development. To fulfill the condition of large TGE selection, we start with 1.8 kV/cm field and 1 km field length subsequently enlarging field strength and extent. As we can see in Fig. 14 at 200 MV potential drop (1 km length of a 2 kV/cm strength field), few RREAs started to develop; at 300 MV potential drop the energy spectra maximal value reaches 20 MeV (Fig. 15), and at 330 MV(Fig. 16) number of avalanche particles exponentially exceeds and maximal energy reaches 40 MeV. As we can see from Figs. 14–16 with enlarging potential drop from 200 to 330 MV the intensity and maximal energy of the electron and gamma ray differential energy spectra abruptly increase. Comparing Figs 14 and 15 with Fig 13 a) and b) we can notice that smaller TGE occurred on 13 May 2012 (enhancement in the SEVAN "100" combination - 9.3% and in STAND1 upper scintillator 22%) can be related to the ≈300 MV potential drop (Fig. 15); maximal energy for simulated and measured energy spectra are ≈ 20 MeV. The larger TGE on 27 May 2014 (enhancement in the SEVAN "100" combination - 12.3% and in STAND1 upper scintillator 31%) in turn can be related to the ≈330 MV potential drop (Fig. 15); maximal energy reaches ≈ 40 MeV. Sure, these relations are only illustrative; the atmospheric electric field is very complicated and our "double dipole" model [41] with fast-changing electric field structure isn't mimicked by the uniform constant electric field assumed in the simulation. Nonetheless, the simulated and measured for these 2 events muon deficits demonstrate the "correct" relation of simulated and measured entities (see Tables 2 and 3).

On the other hand, muon deficits obtained with EXPACS spectra (Section 3) differ from the CORSIKA simulations by1.4% - 3.2% (see Table 3). This difference will lead to a positive bias of 100-150 MV when the method described in Section 3 will be applied to measured muon deficit. Simplified estimates were obtained by shifting energy spectra of positive and negative muons as they were calculated by EXPACS on 3200 MSL height to the left and to the right according to energy gain or loss in the electric field. From the obtained in this way integral spectra the muon deficit was derived by subtracting modified integral spectra from each-other. In this way, we neglect the details of the electromagnetic interactions and

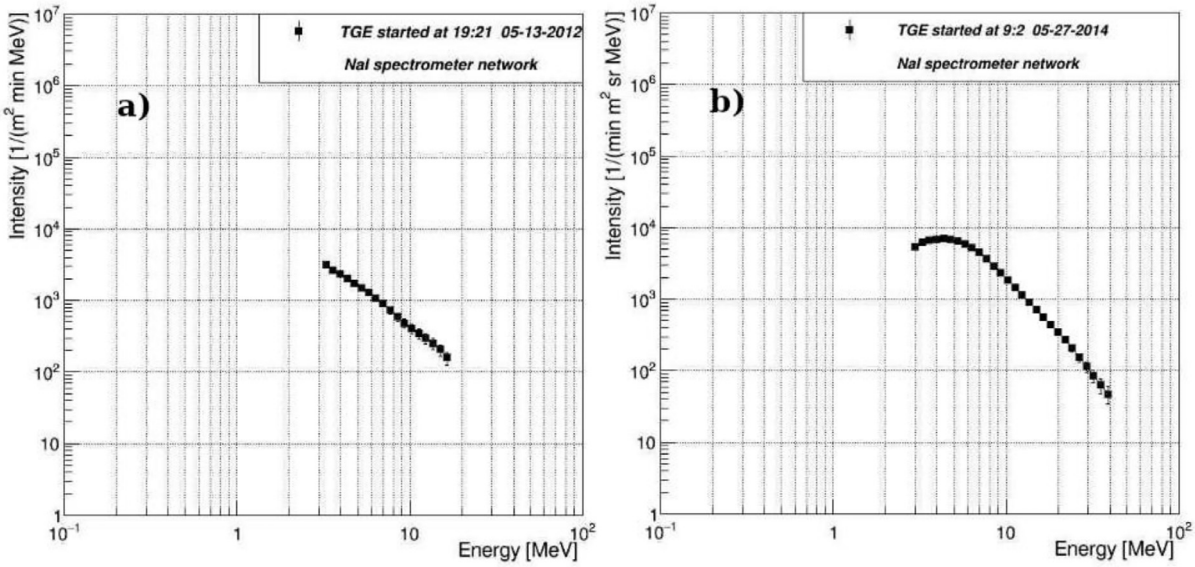

Fig. 13. Differential energy spectra of the TGE events a) and c) measured by NaI spectrometers during the same minute when depletion of the muon flux was registered by SEVAN detector.

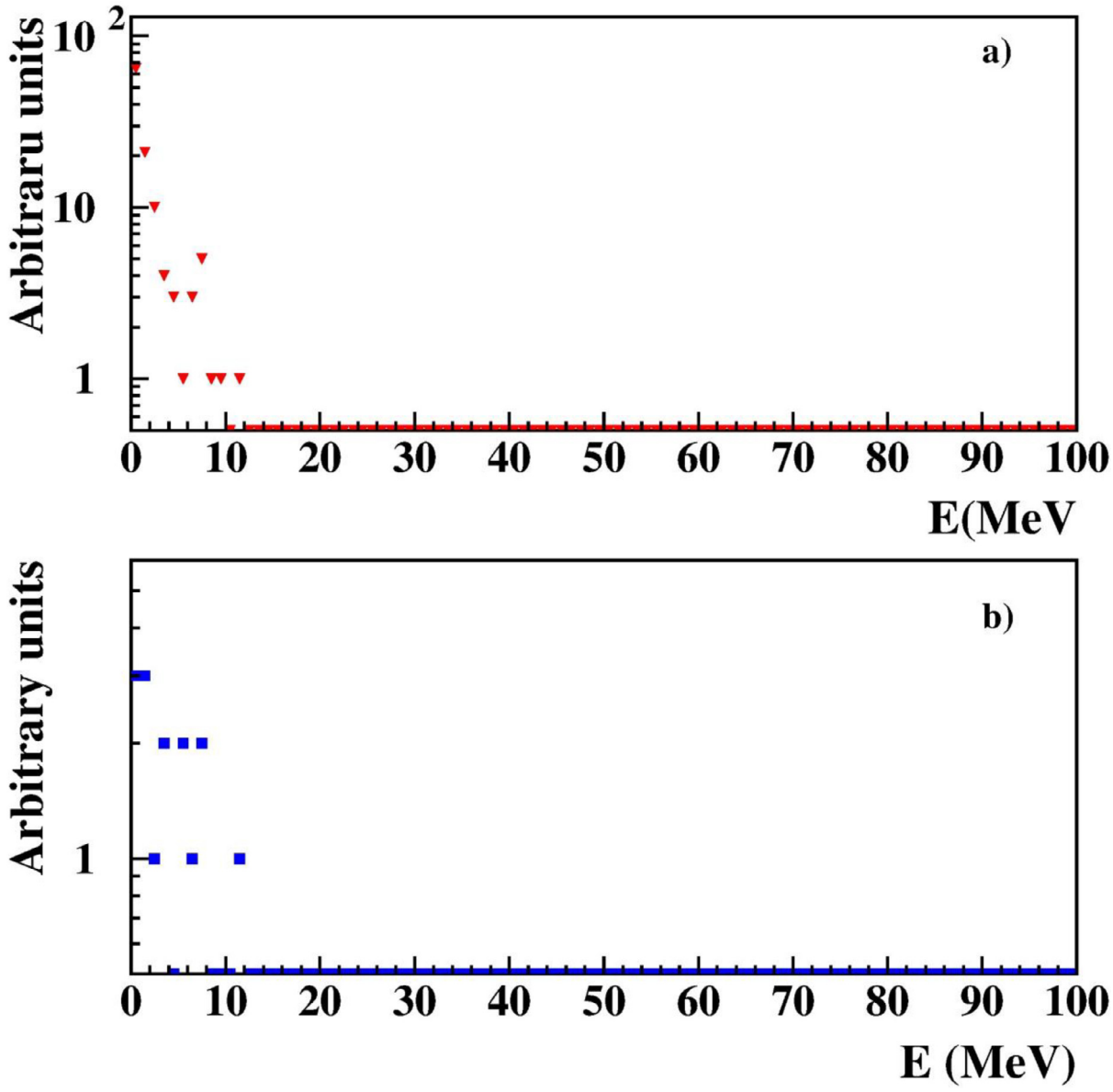

Fig. 14. Differential energy spectra of gamma rays a) and electrons b); potential drop 200 MV, electric field strength – 2 kV/cm, field extent – 1km. Observation level – 3200 m.

Table 3
Number of positive and negative muons after passing the electric field of 2 and 2.2 kV/cm strength, and 1, 1.5 km extent. The numbers of muons reaching 3200 m height are used for calculating the muon deficit.

Simulation conditions	>250MeV	Muon flux changes/%	Muon deficit (%)/Pot. drop (MV)	EXPACS results On muon deficit
$N_{\mu+}$ (Ez=0kV/cm)	24261			
$N_{\mu-}$ (Ez=0kV/cm)	21109			
$N_{\mu+}$ (Ez=2kV/cm, z=1km)	21686	-2248/-5.0	2.3/200	0.8/200
$N_{\mu-}$ (Ez=2kV/cm, z=1km)	22127	1240/2.7		
$N_{\mu+}$ (Ez=2kV/cm, z=1.5km)	20749	-3118/-6.9	3.9/300	2.1/300
$N_{\mu-}$ (Ez=2kV/cm, z=1.5km)	22257	1370/3.0		
$N_{\mu+}$ (Ez=2.2kV/cm, z=1.5km)	20818	-3443/-7.6	4.2/330	2.8/330
$N_{\mu-}$ (Ez=2.2kV/cm, z=1.5km)	22671	1562/3.4		
$N_{\mu+}$ (Ez=2.0kV/cm, z=1.8km)	20462	-3800/-8.4	4.8/360	3.1/360
$N_{\mu-}$ (Ez=2.0kV/cm, z=1.8km)	22738	1629/3.6		
$N_{\mu+}$ (Ez=2.0kV/cm, z=2km)	19681	-4580/-10.0	7.0/400	3.8/400
$N_{\mu-}$ (Ez=2.0kV/cm, z=2km)	22445	1336/3.0		

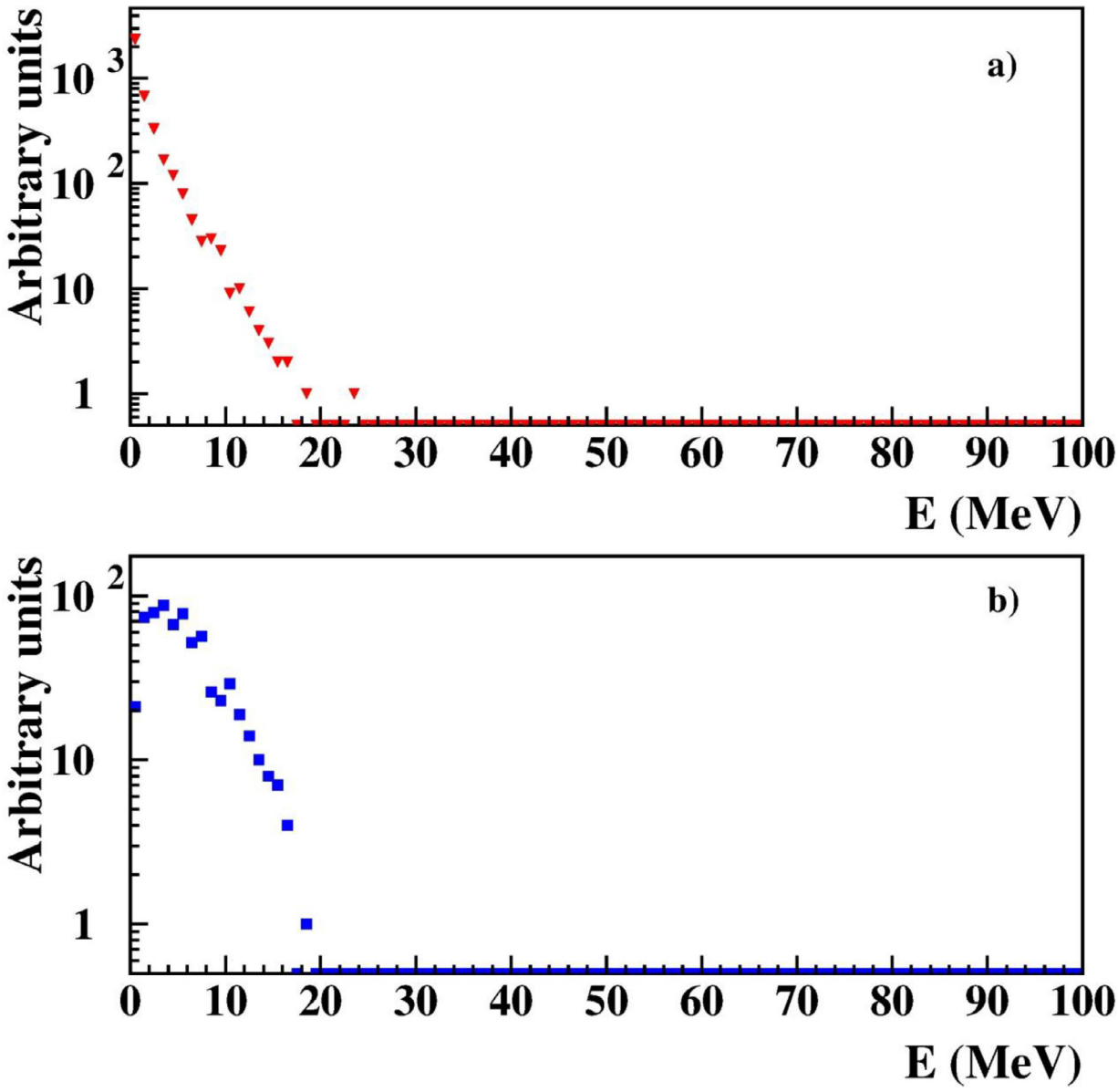

Fig. 15. Differential energy spectra of gamma rays a) and electrons b); potential drop 300 MV, electric field strength – 2 kV/cm, field extent – 1.5km. Observation level – 3200 m.

decay probabilities of positive and negative muons during transport in the electric field. Thus, the passage of muons in the electric field should be treated in all details by the simulation with an appropriate code. CORSIKA made a full simulation of muon transport and on each step of muon propagation, the electromagnetic interactions are applied to the muons with modified (due propagation in the electric field) energies. Therefore, as we demonstrate, CORSIKA results, checked also by gamma ray energy spectra, are trustworthy and can be used to correct the positive bias of EXPACS estimates.

In Table 3 we show results of CORSIKA simulations for different fields and field lengths.

For each potential drop, we calculate the expected muon deficit. In the first column we put the conditions of simulation trials; in the second the number of positive and negative muons with energies above 250 MeV that reach 3200 m height; in the third – the change in overall muon flux and percent of change; in forth - calculated muon deficit and corresponding potential drop; in the last column – results obtained with simple method described in Section 3. In Fig. 17 we show the relation of muon deficit to the potential drop obtained by the CORSIKA simulations with different strength and length of the intracloud electric field. Our calculations are related only to the electric field parameters that can initiate RREA, that was the first condition in the selection of the SEVAN events with muon flux drop. The obtained potential drop interval (200-400 MV) is shifted to the left by 100-150 MV compared with outlined in Fig. 4 for the simplified method, thus the method described in Section 3 is positively biased, i.e., estimate very high potential drops for the same muon deficit comparing with the CORSIKA simulations.

7. Discussion and conclusions

The emergence and evolution of the intracloud electric field and its impact on the high-energy particle flux are among the most important problems of atmospheric physics. Based on the measured intensity and shape of the gamma ray energy spectra a method was proposed for the estimation of the atmospheric electric field

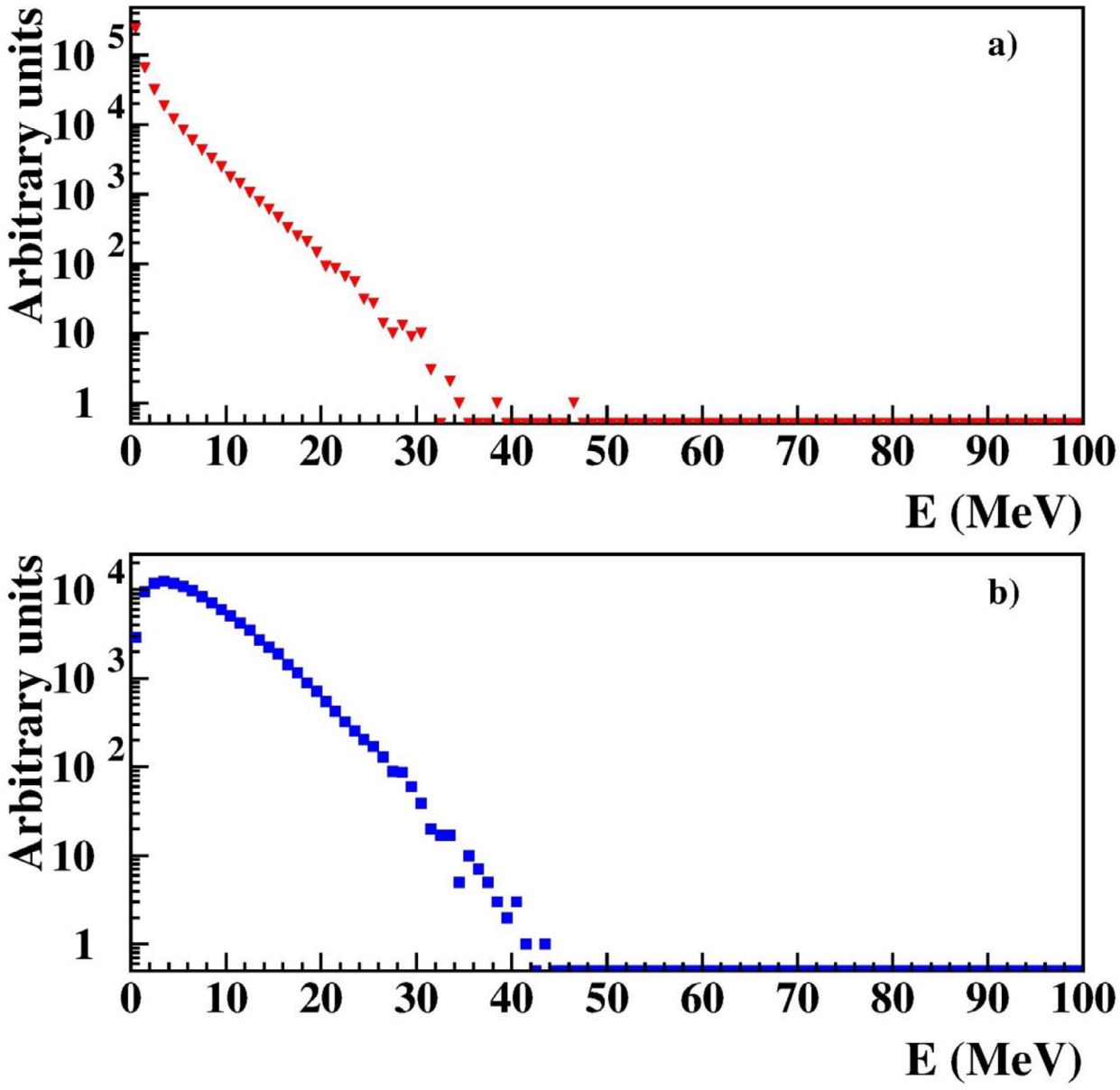

Fig. 16. Differential energy spectra of gamma rays a) and electrons b); potential drop 330 MV, electric field strength – 2.2 kV/cm, field extent – 1km. Observation level – 3200 m.

[42,43]. Now we suggest using additional important information for the electric field estimation. At ASEC different species of cosmic rays are measured along with electric field and meteorological parameters. SEVAN detector, a particle detector belonging to the European network, 7/24 monitoring the muon component of cosmic rays. On Mount Aragats, huge enhancements of electron and γ ray flux were measured simultaneously with the decline of muon flux. The muon deceleration coincides with strong TGEs; the duration of the high-energy part of the TGE usually continued only a few minutes. A lightning flash [44] or a TGE current itself [45] significantly reduced the potential drop and the electric field strength abruptly goes below the threshold level of RREA initiation, also stopping muon deceleration and the further decline of the muon flux. These few minute episodes of large gamma ray/electron enhancement and muon depletion are accompanied as well with inclined muons suppression and emergence of high energy (up to 50 MeV) electrons and gamma rays. Particle fluxes of all species of the cosmic rays are modulated by the atmospheric electric field and registration of energy spectra and intensities of these particles allows to estimate the potential drop and strength of the atmospheric electric field (see Figs 14–17 and Table 3).

Using only muon decline information for the recovering intracloud electric field can lead to erroneous estimates. There is an overall problem of reproducing the number of muons in the simulation of extensive air showers. The measured muon multiplicities disagreement with the modeling at low energies has been reported in several papers, see for instance [46]. The largest variations in muon densities obtained with different models at the ground at the lowest energies (50-250 MeV, energies controlling the muon deficit) resulting from striking differences in the early stages of shower development. Thus, the simulation results are crucially dependent on the energy used spectra and composition of the primary cosmic rays, on the strong interaction model, and on the energy threshold of the detector.

Also, we investigate the muon charge ratio obtained in simulation trials. Both CORSIKA and EXPACS give R=1.15 on 3200 m

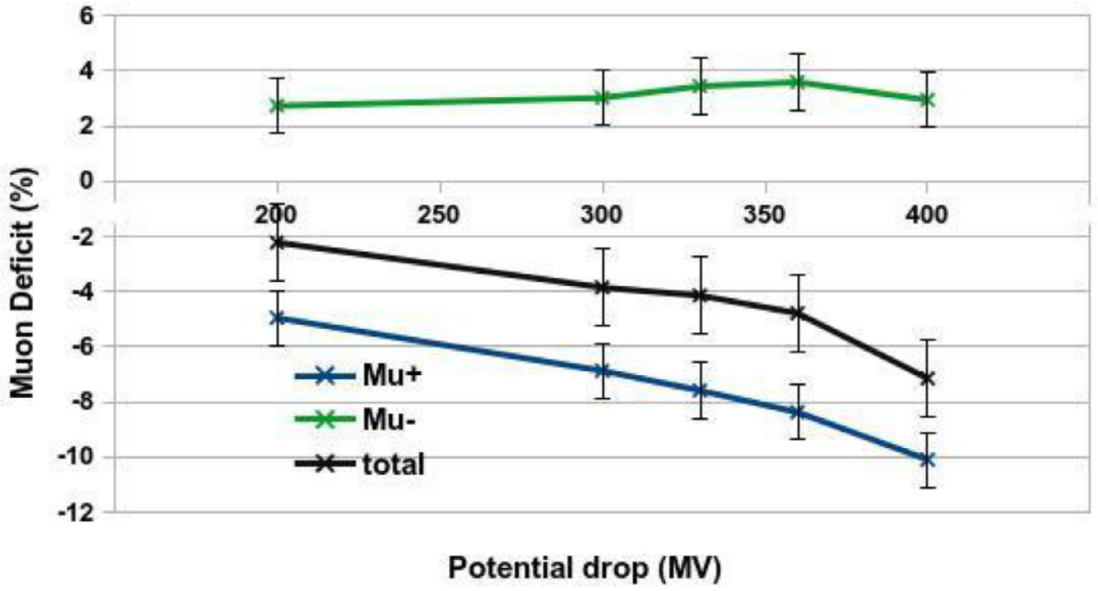

Fig. 17. The potential drop – muon deficit relation for the positive and negative muons and for the sum of both (the analog of the count rate measured by the SEVAN detector). Data from Table 3. Error bars - statistical.

for muons with energies above 250 MeV). The historical measurements of muon charge ration performed on Aragats give consistent values of R=1.29 +/- 0.02 by the vertical magnetic spectrometer [47] (energy threshold – 2.2 GeV) and R=1.28 +/- 0.06 by horizontal magnetic spectrometer [48] (energy threshold 5 GeV), that rather well coincide with a compilation of high-energy atmospheric muon data at sea level, R= 1.268 [49]. Measurements with WILLI detector (Weakly ionizing lead lepton interaction, National Institute of Physics and Nuclear Engineering Bucharest, Romania [50]) also yield a very coherent value of R = 1.27 +/- 0.01 for muons of energies above 0.52 GeV of vertical incidence (mean zenith angle 19°). However, the models of hadronic interactions in the terrestrial atmosphere fail to reproduce such a high charge ratio, giving significantly smaller values of R = 1.15 – 1.20.

Additional simulations with CORSIKA and JEANT4 codes are needed for establishing a decisive relation between the potential drop and muon deficit.

Therefore, our conservative estimate based not only on muon deficit but also on the measured TGE parameters is that for the large TGE events registered on Aragats the maximal potential drop is reaching 350 MV and most probable maximal electric field strength - 2 kV/cm.

Our "multisensory" approach included:

1 Registration of near-surface electric field dropping in negative domain after the active phase of the storm;
2 Registration of large flux of electrons, gamma rays, and neutrons with multiple particle detectors and a simultaneous decline of muon flux;
3 Registration of histograms of energy releases in the network of NaI spectrometers and in 60 cm thick plastic scintillator and the subsequent recovery of differential energy spectra;
4 Registration of simultaneous decline in the intensity of SEVAN "111" combination (~250 MeV muons) and decrease in the muon flux coming from inclined oblique direction observed by the ASNT with simultaneous increase of the flux coming from near-vertical direction;
5 Estimation of the cloud base height above the particle detectors.

In [51], an estimate of the atmospheric electric potential at a height of 8-10 km was obtained based on the measured decline of muon flux. However, independent consideration [52] shows that this estimate was inconsistent, and the reported 1.3 GV potential within a gap of 2 km at 8–10 km altitude above sea level was highly overestimated. Any physical inference based only on data from one detector and neglecting corresponding atmospheric phenomena is highly risky.

Several modules of the European SEVAN network are located on mountain tops and are well suited for the detection of TGEs and the stopping muon effect; recently measured at Lomnitcky Stit (Slovakia) [53] and Musala (Bulgaria) [54] muon decline was more than10%, signaling that the intracloud electric field there is much larger than measured on Aragats. The intensity of particle flux was also extraordinarily high, exceeding the fair-weather level more than 200 times. The mountain tops seem to be truly generators of the huge atmospheric electric fields and the SEVAN detector is an appropriate device for revealing this exciting phenomenon.

Declaration of Competing Interest

We have no conflict of interests related to the paper.

Acknowledgments

We thank the staff of the Aragats Space Environmental Center for safeguarding the operation of experimental facilities on Aragats. The data for this study are available by the multivariate visualization software platform ADEI [55] on the WEB page of the Cosmic Ray Division (CRD) of the Yerevan Physics Institute, http://adei.crd.yerphi.am/adei. The authors would like to thank Suren Chilingaryan for the continuous support of the ADEI knowledge platform highly supporting the online data analysis and physical inference.

References

[1] F.J. Schonland, J.P.T. Viljoen, On a penetrating radiation from thunderclouds, Proc. R. Soc. A 140 (1933) 314.
[2] G.E. Shaw, Background cosmic count increase associated with thunderstorms, J. Geophys. Res. 72 (1967) 4623.
[3] T. Torii, M. Takeishi, T. Hosono, Observation of gamma-ray dose increase associated with winter thunderstorm and lightning activity, J. Geophys. Res. 107 (2002) 4324.

[4] Y. Muraki, Effects of atmospheric electric fields on cosmic rays, Phys.Rev.D 69 (2004) 123010-1-13.
[5] H. Tsuchiya, Observation of an energetic radiation burst from mountain-top thunderclouds, Phys.Rev.Lett. 102 (2009) 255003–255007.
[6] N.S. Khaerdinov, A.S. Lidvansky, V.B. Petkov, Electric field of thunderclouds and cosmic rays: evidence for acceleration of particles (runaway electrons), Atmos. Res. 76 (2005) 346.
[7] A. Chilingarian, A. Daryan, K. Arakelyan, et al., Ground-based observations of thunderstorm-correlated fluxes of high- energy electrons, gamma rays, and neutrons, Phys. Rev. D 82 (2010) 043009.
[8] A. Chilingarian, G. Hovsepyan, A. Hovhannisyan, Particle bursts from thunderclouds: natural particle accelerators above our heads, Phys. Rev. D 83 (2011) 062001.
[9] C.T.R. Wilson, The acceleration of betta-particles in strong electric fields such as those of thunder-clouds, Proc. Camb. Philos. Soc. 22 (1924) 534.
[10] A.V. Gurevich, G. Milikh, R. Roussel-Dupre, Runaway electron mechanism of air breakdown and preconditioning during a thunderstorm, Phys. Lett. A 165 (1992) 463.
[11] V.V. Alexeenko, N.S. Khaerdinov, A.S. Lidvansky, et al., Transient variations of secondary cosmic rays due to atmospheric electric field and evidence for pre–lightning particle acceleration, Phys. Lett. A 301 (2002) 299.
[12] A.S. Lidvansky, N.S. Khaerdinov, Parameters of particle fluxes generated by GCR in thunderstorm electric fields, Bull. Russ. Acad. Sci. 73 (2009) 400, doi:10.3103/S1062873809030368.
[13] J.M. Baxendale, C.J. Hume, M.G. Thompson, Precise measurement of the sea level muon charge ratio, J. Phys. G 1 (1975) 781.
[14] SMS collaboration, Measurement of the charge ratio of atmospheric muons with the CMS detector, Phys. Lett. B 692 (2010) 83, doi:10.1016/j.physletb.2010.07.033.
[15] L.I. Dorman, A.A. Lagutin, G.V. Chernyaev, Proc. 21st ICRC, , 7 (1990) 81.
[16] P.V. Mironychev, Cosmic ray muons in thunderous electrified clouds, Geomagn. Aeron. 43 (5) (2003) 702.
[17] A.S. Lidvansky, N.S. Khaerdinov, Strong variations of cosmic ray muons during thunderstorms, Bull. Russ. Acad. Sci. 73 (2009) 3, doi:10.3103/S1062873809030356.
[18] N.S. Khaerdinov, Strong enhancement of cosmic ray intensity during thunderstorm: a case study and implications, in: Proc. 29th International Cosmic Ray Conference, 2, Pune, 2005, p. 393. v..
[19] J. Kuettner, The electrical and meteorological conditions inside thunderclouds, J. Meteorol. 7 (1950) 322.
[20] T.C. Marshall, M.P. McCarthy, W.D. Rust, Electric field magnitudes and lightning initiation in thunderstorms, J. Geophys. Res. 100 (1995) 7097–7103, doi:10.1029/95JD00020.
[21] T.C. Marshall, T. C., M. Stolzenburg, C.R. Maggio, et al., Observed electric fields associated with lightning initiation, Geophys. Res. Lett. (2005) L03813, doi:10.1029/2004GL021802.
[22] E.R. Williams, The tripole structure of thunderstorms, JGR 94 (1989) 151-13,167.
[23] E.R. Williams, R. Zhang, J. Rydock, Mixed-phase microphysics and cloud electrification, J. Atmos. Sci. 48 (1991) 2195 1991.
[24] G. Karapetyan, Variations of muon flux in the atmosphere during thunderstorms, Phys. Rev. D 89 (2014) 093005.
[25] A. Chilingarian, K. Arakelyan, K. Avakyan, V. Babayan, et al., Correlated measurements of secondary cosmic ray fluxes by the Aragats space-environmental center monitors, NIM A 543 (2–3) (2005) 483.
[26] A. Chilingarian, N. Bostanjyan, T. Karapetyan, L. Vanyan, Remarks on recent results on neutron production during thunderstorms, Phys. Rev. D 86 (2012) 093017.
[27] A. Chilingarian, N. Bostanjyan, T. Karapetyan, On the possibility of location of radiation-emitting region in thundercloud, J. Phys. Conf. Ser. 409 (2013) 012217.
[28] A. Chilingarian, V. Babayan, T. Karapetyan, et al., The SEVAN Worldwide network of particle detectors: 10 years of operation, Adv. Space Res. 61 (2018) 2680.
[29] T. Sato, Analytical model for estimating the zenith angle dependence of terrestrial cosmic ray fluxes, PLoS One 11 (8) (2018) e0160390.
[30] A. Chilingarian, G. Hovsepyan, A. Elbekian, T. Karapetyan, L. Kozliner, H. Martoyan, B. Sargsyan, Origin of enhanced gamma radiation in thunderclouds, Phys. Rev. Res. 1 (2019) 033167.
[31] A. Chilingarian, G. Hovsepyan, B. Mailyan, In situ measurements of the runaway breakdown (RB) on Aragats mountain, NIM A 19 (2017) 874.
[32] A. Chilingarian, S. Chilingaryan, G. Hovsepyan, Calibration of particle detectors for secondary cosmic rays using gamma-ray beams from thunderclouds, Astropart. Phys. 69 (2015) 37.
[33] E.K. Svechnikova, N.V. Ilin, E.A. Mareev E.A., et al., Characteristic features of the clouds producing thunderstorm ground enhancements, submitted to JGR, 2020.
[34] D. Heck, J. Knapp, A Monte Carlo Code to Simulate Extensive Air Showers, Forschungszentrum Karlsryhe, FZKA Report 6019, 1998.
[35] N.N. Kalmykov, S.S. Ostapchenko, A.I. Pavlov, Quark-gluon-string model and EAS simulation problems at ultra-high energies, Nucl. Phys. B 52B (17) (1997) (Proc. Suppl.).
[36] S.A. Bass, et al., Microscopic models for ultrarelativistic heavy ion collisions, Prog. Part. Nucl. Phys. 41 (1998) 225.
[37] W.R. Nelson, H. Hirayama, and D.W.O. Rogers, The EGS4 Code System, Report SLAC 265 (1985), Stanford Linear Accelerator Center.
[38] E. Sveshnikova, N. Ilin, E. Mareev, Recovery of electric structure of the cloud with use of ground-based measurement results, in: Proceedings of 8-th TEPA Symposium, Nor-Amberd-2018, 2019, p. 75. Tigran Mets.
[39] M. Verderi, A. Walkden, J.P. Wellisch, D.C. Williams, D. Wright, H. Yoshida, Geant4 developments and applications, IEEE Trans. Nucl. Sci. 53 (1) (2006) 270–278.
[40] A. Chilingarian, G. Hovsepyan, S. Soghomonyan, M. Zazyan, M. Zelenyy, Structures of the intracloud electric field supporting origin of long-lasting thunderstorm ground enhancements, Phys. Rev. 98 (2018) 082001.
[41] A. Chilingarian, G. Hovsepyan, T. Karapetyan, et al., Structure of thunderstorm ground enhancements, PRD 101 (2020) 122004.
[42] A. Chilingarian, G. Hovsepyan, Y. Khanikyanc, A. Reymers, S. Soghomonyan, Lightning origination and thunderstorm ground enhancements terminated by the lightning flash, Europhys. Lett. 110 (2015) 49001.
[43] E.S. Cramer, B.G. Mailyan, S. Celestin, J.R. Dwyer, A simulation study on the electric field spectral dependence of thunderstorm ground enhancements and gamma ray glows, J. Geophys. Res. Atmos. 122 (2017) 4763, doi:10.1002/2016JD026422.
[44] A. Chilingarian, S. Chilingaryan, T. Karapetyan, et al., On the initiation of lightning in thunderclouds, Scientific Reports 7, Article number: 1371, (2017).
[45] A. Chilingarian, Y. Khanikyants, V.A. Rakov, S. Soghomonyan, Termination of thunderstorm-related bursts of energetic radiation and particles by inverted-polarity intracloud and hybrid lightning discharge, Atmos. Res. 233 (2020) 104713.
[46] R.D. Parsons, H. Schoorlemmer, Systematic differences due to high energy hadronic interaction models in air shower simulations in the 100 GeV-100 TeV range, Phys. Rev. D 100 (2019) 023010.
[47] N.M. Kocharyan, Z.A. Kirakosyan, G.S. Saakyan, energy spectra and nuclear interactions of cosmic ray particles, JETF 35 (1958) 1335.
[48] T.L. Asatiani, S.V. Alchudgian, K.A. Gazaryan, et al., Momentum spectrum and charge ratio of cosmic ray muons at zenith angle 84°, in: Proceedings of 15-th ICRC, 11, Plovdiv, Bulgaria, 1977, pp. 362–367.
[49] T. Hebbeker, C. Timmermans, A compilation of high energy atmospheric muon data at sea level, Astropart. Phys. 18 (2002) 107–127.
[50] B. Vulpescu, The Cosmic Ray Muon Charge Ratio, Forschungszentrum Karlsruhe, preprint FZKA 6368.
[51] B. Hariharan, A. Chandra, S.R. Dugad, et al., Measurement of the electrical properties of a thundercloud through muon imaging by the GRAPES-3 experiment, Phys. Rev. Lett. 122 (2019) 105101.
[52] A. Chilingarian, G. Hovsepyan, E. Svechnikova, E. Mareev, Comment on "Measurement of the electrical properties of a thundercloud through muon imaging by the GRAPES-3 experiment, PRL 124 (2020) 019501.
[53] J. Chum, R. Langer, J. Baše, M. Kollárik, I. Strhárský, G. Diendorfer, J. Rusz, Significant enhancements of secondary cosmic rays and electric field at high mountain peak during thunderstorms, Earth Planets Space 72 (2020) 28.
[54] N. Nikolova, Pravite communication, http://www.crd.yerphi.am/adei/.
[55] S. Chilingaryan, A. Chilingarian, V. Danielyan, W. Eppler, The Aragats data acquisition system for highly distributed particle detecting networks, J. Phys. Conf. Ser. 119 (2008) 082001.